Available online at www.sciencedirect.com

SciVerse ScienceDirect

Ceramics International 39 (2013) 4171–4178

CERAMICS INTERNATIONAL

www.elsevier.com/locate/ceramint

Ablation behavior and mechanism of C/C–ZrC–SiC composites under an oxyacetylene torch at 3000 °C

Jing Xie, Kezhi Li*, Hejun Li, Qiangang Fu, Lingjun Guo

State Key Laboratory of Solidification Processing, Carbon/Carbon Composites Research Center, Northwestern Polytechnical University, Xi'an 710072, PR China

Received 29 August 2012; received in revised form 23 October 2012; accepted 31 October 2012
Available online 8 November 2012

Abstract

C/C–ZrC–SiC composites with continuous ZrC–SiC ceramic matrix were prepared by a multistep technique of precursor infiltration and pyrolysis process. Ablation properties of the composites were tested under an oxyacetylene flame at 3000 °C for 120 s. The results show that the linear ablation rate of the composites was about an order lower than that of pure C/C and C/C–SiC composites as comparisons, and the mass of the C/C–ZrC–SiC composites increased after ablation. Three concentric ring regions with different coatings appeared on the surface of the ablated C/C–ZrC–SiC composites: (i) brim ablation region covered by a coating with layered structure including SiO_2 outer layer and ZrO_2–SiO_2 inner layer; (ii) transition ablation region, and (iii) center ablation region with molten ZrO_2 coating. Presence of these coatings which acted as an effective oxygen and heat barrier is the reason for the great ablation resistance of the composites.

Keywords: C. Corrosion; E. Thermal applications; C/C–ZrC–SiC composites

1. Introduction

Carbon/carbon (C/C) composites exhibit a unique combination of low density, low coefficiency of thermal expansion, excellent high-temperature strength, high thermal conductivity, great ablation and thermal shock resistance [1,2]. These outstanding properties make them as the leading structural materials used in high temperature environment such as rocket engines, nose tips, leading edges and other thermal protection systems for space vehicles [3–5]. The operation temperatures of these components may increase rapidly from room temperature to over 3000 °C and last from several seconds to several hundred seconds. However, C/C composites are vulnerable to be ablated at ultrahigh temperature (over 2000 °C) and high-speed gas jet and particle erosion (usually supersonic velocity), which restricts their potential application in new type and high performance aerospace vehicles along with the great development of aerospace sector [6,7]. Thus, improving ablation resistance at ultrahigh temperature in oxygen-containing environment is a challenge to extend applications of C/C composites.

It has been proved that introducing ultrahigh temperature ceramics (UHTCs) including transition metal borides and carbides into C/C matrix is one of the widely used methods to improve the ablation resistance of C/C composites [8–10]. In the last few years, many efforts have been made to develop C/C–UHTC composites [11–13]. However, most of the works were focused on UHTC modified C/C composites, and the UHTC contents in these composites were low. Therefore, the improvement of ablation resistance of C/C composites was limited. Recently, C/C–ZrC–SiC [14–17] composites with large amounts of ZrC and SiC which can form a continuous ceramic matrix were prepared by precursor infiltration and pyrolysis (PIP) process using organic precursor. It was found that the use of organic precursor to introduce UHTCs into C/C composites could improve not only the content but also the distribution homogeneity of UHTC phases in the composites. However, these reports mainly concentrated on fabrication and mechanical properties of C/C–ZrC–SiC

---

*Corresponding author. Tel.: +86 29 88495764; fax: +86 29 88495764.
E-mail address: likezhi@nwpu.edu.cn (K. Li).

0272-8842/$ - see front matter © 2012 Elsevier Ltd and Techna Group S.r.l. All rights reserved.
http://dx.doi.org/10.1016/j.ceramint.2012.10.273

composites, and ablation behavior and mechanism of the composites were not investigated in detail.

In the present work, C/C–ZrC–SiC composites were prepared by PIP process using the mixture solution of organic zirconium-containing polymer (PZC) and polycarbosilane (PCS) as precursor. The main objective of this work was to determine the effects of ablation at different regions by oxyacetylene torch test with a flame temperature about 3000 °C, and the ablation mechanism was proposed.

2. Experimental

2.1. Fabrication of the composites

The schematic preparation procedure of C/C–ZrC–SiC composites was shown in Fig. 1. Firstly, 2D needled carbon fiber felts with a density of 0.45 g/cm^3 (Yixing Tianniao High Technology Co., Ltd, Jiangsu, China) were densified through thermal gradient chemical vapor infiltration (TCVI) process to porous C/C composites with a density of 0.9 g/cm^3. PZC (Institute of Process Engineering, Chinese Academy of Sciences, Beijing, China) and PCS (National University of Defense Technology, Changsha, China) were mixed with a weight ratio of 3:1 [15] and dispersed in dimethylbenzene to form a homogenous solution, using as ZrC–SiC precursor. The PZC consists of four elements including C, H, O, and Zr, and the ceramic productivity is about 28%. Then, C/C–ZrC–SiC composites were fabricated by 12 cycles of infiltration with ZrC–SiC precursor into the porous C/C composites, drying in a drying oven, and heat treatment at 1500 °C for 2 h at an argon atmosphere. Meanwhile, pure C/C and C/C–SiC composites were fabricated by TCVI and PIP process, respectively, under the same conditions for comparisons. The density and open porosity of the C/C–ZrC–SiC composites were 2.22 g/cm^3 and 19.70%, and those of pure C/C composites were 1.75 g/cm^3 and 9.03%, respectively. The density and open porosity of the C/C–SiC composites were 1.90 g/cm^3 and 8.57%, respectively.

2.2. Ablation tests

According to GJB322A-96 standard [18], ablation properties of C/C–ZrC–SiC composites were carried out in oxyacetylene torch with cylindrical-shaped specimens (∅30 mm × 10 mm). The pressure and flux of acetylene were 0.095 MPa and 0.31 L/s, and 0.4 MPa and 0.42 L/h for oxygen, respectively. The temperature of oxyacetylene flame was about 3000 °C and that of the center ablation surface of the composites was measured by an optical pyrometer. The inner diameter of the oxyacetylene gun tip was 2 mm and the distance between the gun tip and the specimen was 10 mm. The specimens were fixed in a water-cooled copper concave, and exposed to the flame for 120 s. Both the linear and mass ablation rates were calculated by thickness and mass change before and after ablation test of each specimen. The final ablation rates of the composites were the average results of three specimens.

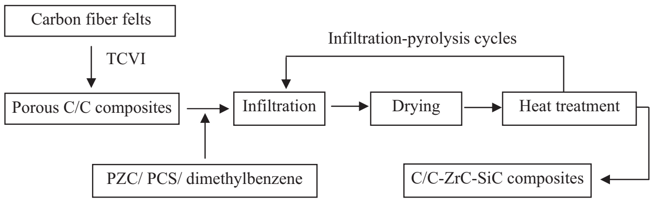

Fig. 1. Schematic preparation procedures of C/C–ZrC–SiC composites.

2.3. Mechanical tests

Three-point-bending tests were performed on an electronic universal testing machine (CMT 5304, Suns Co. China) to determine the mechanical properties of C/C–ZrC–SiC composites. The tests were carried out with a load velocity of 0.05 mm/min at room temperature. The effective size of the sample was 55 mm × 10 mm × 4 mm, and five samples were used for each test.

2.4. Specimen characterization

Density and open porosity of the obtained composites were measured by Archimedes method. Each data point was an average of three values. Phase analysis of the composites was carried out by X-ray diffraction (XRD, Philips X'Pert MPD) using Cu as anode material. The microstructure and morphology of the composites before and after ablation were investigated by scanning electron microscopy (SEM, VEGA TS5136XM) equipped with an energy dispersive spectroscopy (EDS).

3. Results and discussion

3.1. Microstructure characterization

Fig. 2 shows the backscattered electron images and XRD pattern of cross sections of the obtained composites. XRD pattern (Fig. 2(d)) shows that phases in the composites are Carbon, ZrC and SiC, which indicates that the PZC and PCS are transformed into ZrC and SiC, respectively, without any impurity phase. In Fig. 2(a), ceramic fillers mainly concentrate in short-cut fiber webs between non-woven layers, and form deeply along the vertical direction of the fiber webs. ZrC–SiC ceramic fills in the gaps between carbon fiber bundles, and it seems not very dense (Fig. 2(b)), attributing to the escape of gases during the pyrolysis process of PZC and PCS. As seen in Fig. 2(c), the carbon fibers are first surrounded by a pyrolytic carbon layer which can increase preform stiffness and prevent damage to the fibers in the subsequent processing, and the bright-white ZrC particles are imbedded in the dark-gray SiC matrix uniformly.

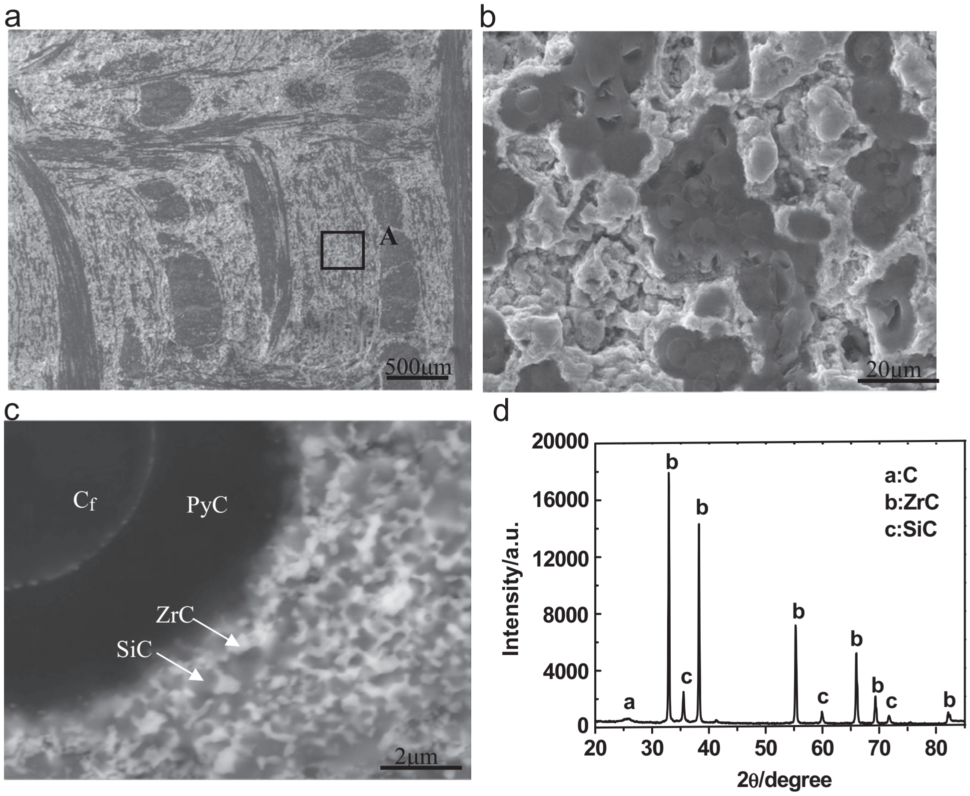

Fig. 2. Backscattered electron images and XRD pattern of the cross sections C/C–ZrC–SiC composites before ablation: (a) low magnification; (b) high magnification of area A in (a); (c) PyC, ZrC, and SiC around carbon fiber; and (d) XRD pattern.

Table 1
Ablation and mechanical properties of the obtained composites.

Materials	Content of ZrC (vol%)	Content of SiC (vol%)	Linear ablation rate ($\times 10^{-3}$ mm/s)	Mass ablation rate ($\times 10^{-4}$ g/s)	Flexural strength (Mpa)
C/C–ZrC–SiC	12.20	16.38	2.48	−3.75	128.37
Pure C/C	–	–	27.30	21.80	126.85
C/C–SiC	–	31.25	30.00	44.04	141.77

3.2. Mechanical and ablation properties

Ablation properties of C/C–ZrC–SiC composites are listed in Table 1. The linear ablation rate of the composites is 2.48×10^{-3} mm/s, which is about an order lower than that of pure C/C and C/C–SiC composites. The negative mass ablation rate of C/C–ZrC–SiC composites indicates weight gain after ablation. It also can be seen from the table that flexural strength of the composites is 128.37 MPa which is at the same level of pure C/C, and it is lower than that of C/C–SiC composites.

Fig. 3(a) shows surface appearance photograph of C/C–ZrC–SiC composites after ablation for 120 s. According to the appearance difference, the surface of the ablated composites can be divided into three concentric ring regions (center ablation region, transition ablation region, and brim ablation region). The center region is covered with a white dense coating, though there is a small ablation crater in the centermost area. Some carbon fibers and matrix can be observed due to the peeling-off of the white layer. There is a mixture of white and gray coating on the transition ablation region, while only gray coating covers the brim ablation region. The temperature of center ablation surface is in excess of 2400 °C, as seen in Fig. 3(b).

3.3. Ablation morphology

3.3.1. Brim ablation region

Fig. 4 shows SEM micrographs of brim ablation region of C/C–ZrC–SiC composites. Fig. 4(a) indicates that the ablated surface is covered with a dense coating with irregular grains. The average size of the grains is approximately 5 μm. According to Fig. 4(c), this layer is composed of Si and O, which confirms that it is SiO_2. Carbon fibers and carbon matrix are not observed. The cross-section of the ablated composites in the brim region provides insight

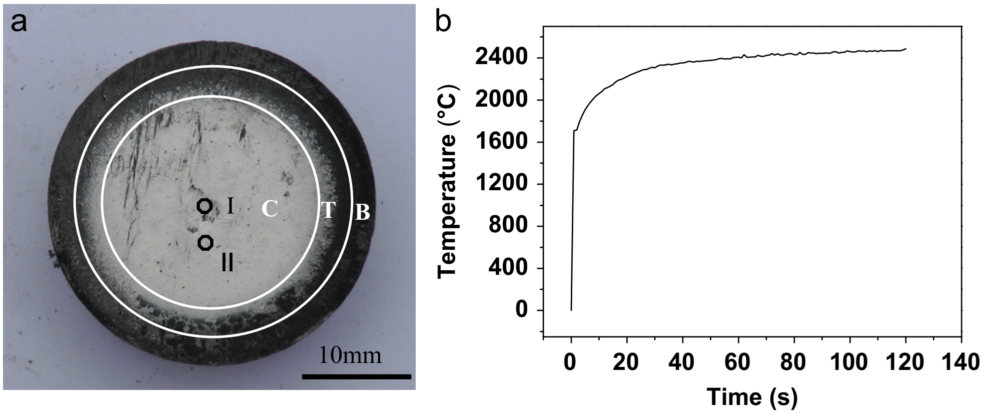

Fig. 3. (a) Surface appearance photograph of C/C–ZrC–SiC composites ablated by oxyacetylene torch for 120 s (C, center region; *T*, transition region; *B*, brim region), and (b) measured result of temperature curve of the center ablation surface.

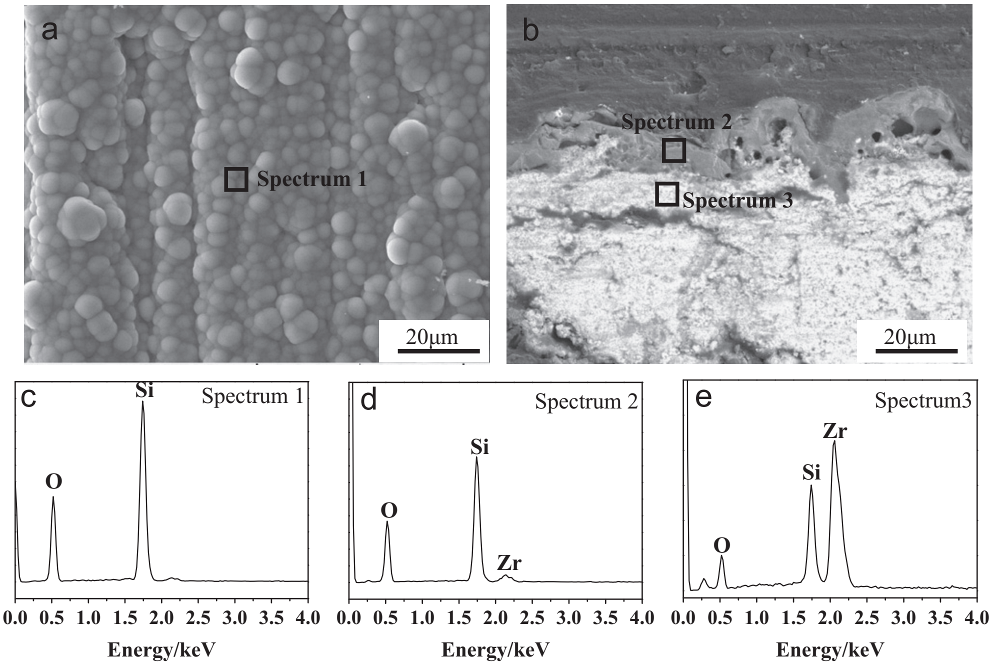

Fig. 4. SEM micrographs and EDS analysis of brim ablation region of C/C–ZrC–SiC composites: (a) surface; (b) cross section; (c), (d), and (e) EDS analysis.

into the microstructure details (Fig. 4(b)). Combined with EDS analysis (Fig. 4(d) and (e)), it is significant to note that the coating in this region consists of two distinct layers: a dense SiO_2 layer with a thickness about 8 μm and an oxidized zone composed of ZrO_2 and a little SiO_2. There are some pores in the interface of these two layers due to the release of gases produced during ablation process. Ablation is not very serious as the temperature and the combustion gas impact in this area are the lowest in all of the three regions. The SiO_2 outer layer can resist the ablative environment effectively.

3.3.2. *Transition ablation region*

As seen in Fig. 5(a), (c) and (d), transition ablation region is covered with a coating mixed of ZrO_2 and SiO_2. Fig. 5(b) shows the high magnification of this region, which demonstrates SiO_2 outer layer coating on the ZrO_2–SiO_2 inner layer, and it is partly damaged during the ablation and the inner layer appears. The temperature in the transition ablation region is higher than that in the brim region. At this temperature, SiO_2 shows a very low viscosity and significant evaporation rate. Thus, it would be easily blown away by the impact of combustion gas.

3.3.3. *Center ablation region*

Fig. 6 shows SEM micrographs and EDS analysis of center ablation region of C/C–ZrC–SiC composites. From EDS analysis, it can be seen that the coating covered on the center ablation region is mainly composed of ZrO_2 generated from the oxidation of ZrC. SiO_2 is not detected

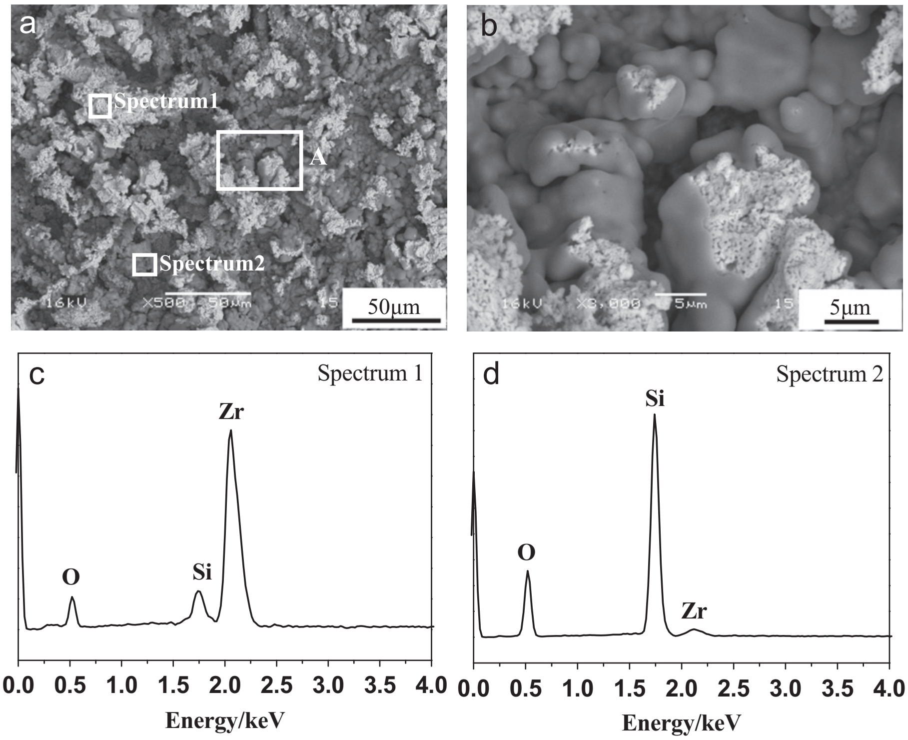

Fig. 5. SEM micrographs and EDS analysis of transition ablation region of C/C–ZrC–SiC composites: (a) low magnification; (b) high magnification of area A in (a); (c) and (d) EDS analysis.

on the ablated surface. Two kinds of ZrO_2 morphologies are found in this region, as shown in Fig. 6(a) and (b). Fig. 6(a) shows the high magnification of the centermost area (area I in Fig. 3) in the center ablation region, from which it can be seen that the ZrO_2 layer have been molten completely. Micro-cracks and voids are observed on the surface. The ZrO_2 layer, as shown in Fig. 6(b), seems rugged. Actually, it is a kind of molten structure with molten ZrO_2 grains adherent to each other closely (Fig. 6(c)). The forming of different morphology of ZrO_2 is attributing to the inhomogeneous temperature distribution of oxyacetylene torch flame. It should be noted that the present testing temperature is almost 300 °C lower than the melting point of ZrO_2 (2677 °C) [19]. The reason for the formation of this molten ZrO_2 layer is that the solution of SiO_2 in ZrO_2 can result in a lower melting point of ZrO_2 [20]. Besides, there is a real possibility that the molten ZrO_2 is formed below the melting point by sintering. According to the cross-section micrographs of this region (Fig. 6(d)) and its EDS analysis (Fig. 6(f)), it conforms that the coating formed in this region on the surface of the composites is mainly composed of ZrO_2 and there are few SiO_2 existing under the outermost layer. The above observation and analysis suggest that the molten ZrO_2 layer has rather high viscosity and strong adhesion to the C/C–ZrC–SiC composites. It is difficult to be blown away by the gas flow, which would prevent the composites from further oxidation at ultrahigh temperature in the center ablation region. Besides, the ZrO_2 layer can serve as a barrier to retard oxygen and thermal diffusion, which can reduce heat transfer and oxygen transport to the underlying material.

3.4. Ablation mechanism

Ablation is an erosive phenomenon with a removal of material by the combination of thermo-mechanical, thermo-chemical, and thermo-physical factors from high temperature, pressure, and velocity of combustion flame [21]. The above analysis of different ablation regions may give some understanding of the ablation mechanism of the C/C–ZrC–SiC composites. The reactions occurred during the oxyacetylene torch ablation process are as follows:

$$2SiC(s)+3O_2(g)=2SiO_2(l)+2CO(g) \quad (1)$$

$$SiC(s)+O_2(g)=SiO(g)+CO(g) \quad (2)$$

$$SiO_2(l)+CO(g)=SiO(g)+CO_2(g) \quad (3)$$

$$SiO_2(l)=SiO_2(g) \quad (4)$$

$$2C(s)+O_2(g)=2CO(g) \quad (5)$$

$$C(s)+O_2(g)=CO_2(g) \quad (6)$$

$$ZrC(s)+3O_2(g)=2ZrO_2(s)+2CO(g) \quad (7)$$

$$ZrO_2(s)=ZrO_2(l) \quad (8)$$

When ablation gases reach the surface of the composites, the temperature of the composites will rapidly increase and the oxidative gases will react with carbon fibers, carbon

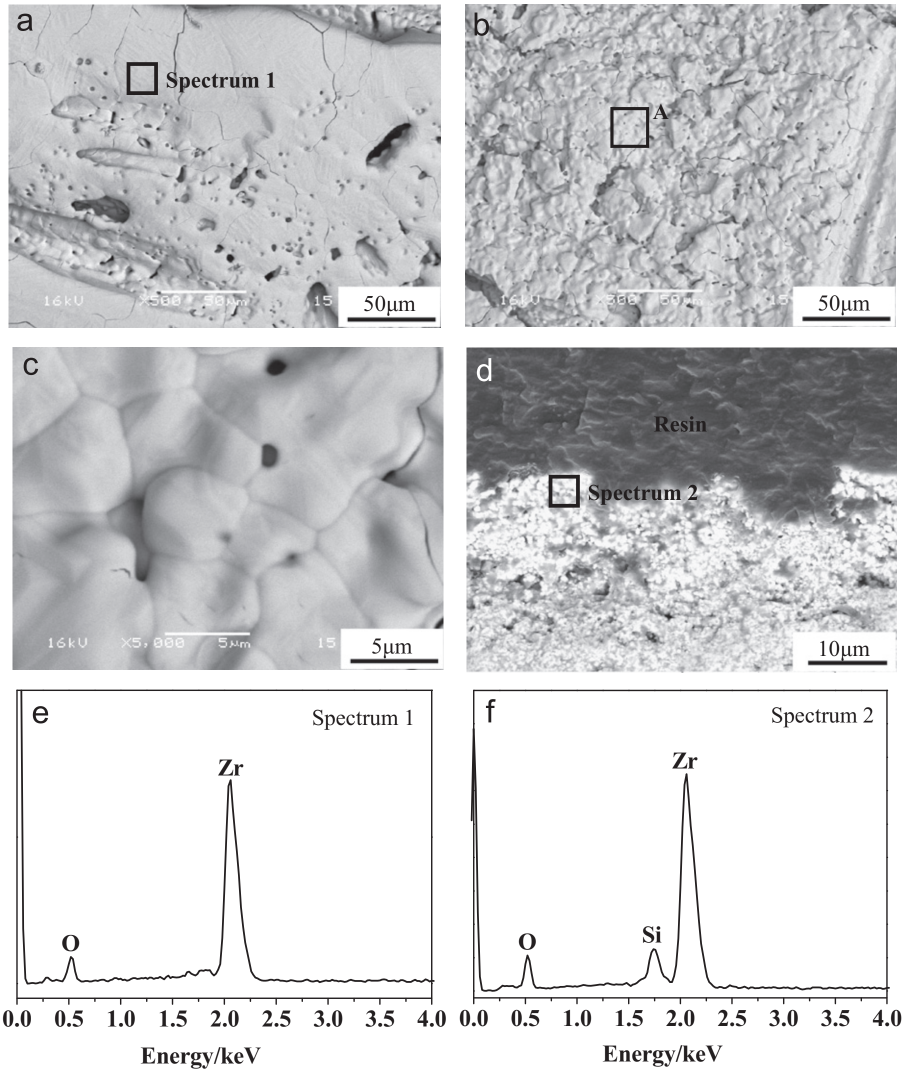

Fig. 6. SEM micrographs and EDS analysis of center ablation region of C/C–ZrC–SiC composites: (a) and (b) high magnification of area I and II in Fig. 3, respectively; (c) high magnification of area A in Fig. 6(b); (d) cross section; (e) and (f) EDS analysis.

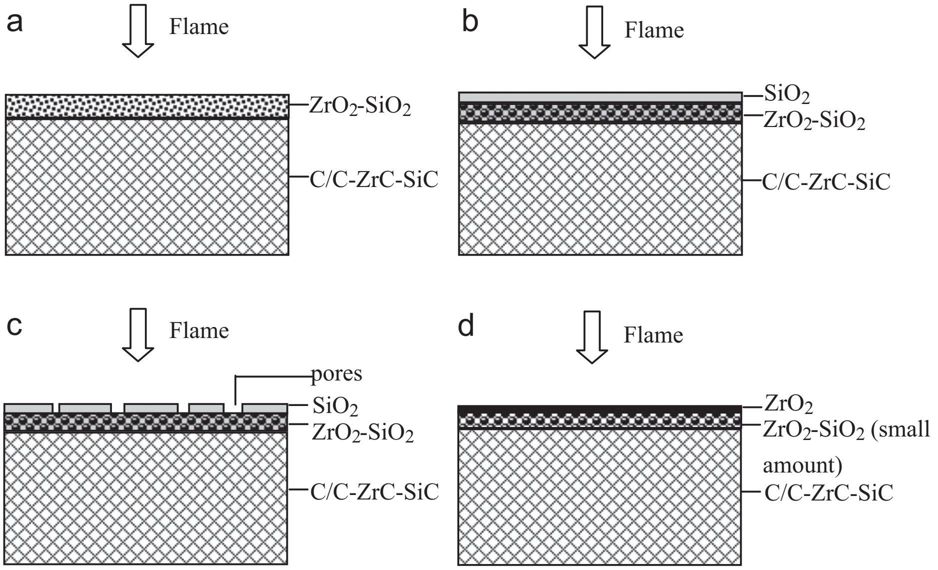

Fig. 7. Schematic of the oxyacetylene ablation process of C/C–ZrC–SiC composites.

matrix, ZrC and SiC, respectively. Thermal chemical erosion happens according to reactions (1)–(3) and (5)–(7). An oxidized layer which consists of ZrO_2 and SiO_2 forms on the surface of the composites (Fig. 7(a)). With the ablation process going, more and more gases such as CO and CO_2 forms in the oxidized layer. Thus, the vapor pressure in the oxidized layer exceeds the sum of the ambient pressure and the tensile force of this layer. The melting point of SiO_2 is only 1670 °C, so it melts (reaction (4)). As a result of the vapor pressure, the molten SiO_2 is forced out from the oxidized layer to the surface of the composites. Therefore, the layered structure of SiO_2 outer layer and ZrO_2–SiO_2 inner layer forms (Fig. 7(b)). The formation of SiO_2 outer layer is similar to that of SiO_2-rich glass layer in the oxidation process of ZrB_2–SiC–ZrC ceramic [22]. The ablation rate is originally controlled by the rapid chemical reaction of the surface carbon, ZrC and SiC with oxygen and then controlled by the diffusion rate of oxygen through protective layer on the surface of composites.

In the brim ablation region, the temperature and gas pressure are relatively low. SiO_2 outer layer can resist the oxidizing environments. While, in the transition ablation region, the temperature and pressure increase significantly. So, the SiO_2 outer layer would evaporate or be eroded away partly by the combustion gas, leaving a few pores or craterlets on the SiO_2 layer (Fig. 7(c)). The center region is faced with the core of the oxyacetylene flame and its ablation is the most serious in the three regions. As indicated by the pyrometer, the temperature of composite surface is about 2400 °C. However, SiO_2 is thermochemically stable below 1800 °C and will lose its protective effect at temperatures above 2300 °C [23] attributing to reactions (1), (3) and (4). ZrO_2 with relative low vapor pressure and high viscosity is more stable at temperature excess 2000 °C. It becomes liquid (reaction (8)), providing a sealing mechanism to fill the interspaces, cracks, and pores in matrix and obstruct the diffusing channels of the ablative flame (Fig. 7(d)).

4. Conclusions

C/C–ZrC–SiC composites with great amounts of ZrC and SiC were fabricated by PIP process using PZC and PCS. After ablation for 120 s, the composites exhibited a good ablation resistance with the linear and mass ablation rates of 2.48×10^{-3} mm/s and -3.75×10^{-4} g/s, respectively. Three concentric ring regions appeared on the surface. In the brim ablation region where the temperature and gas pressure were lower, a layered coating consisted of SiO_2 outer layer and ZrO_2–SiO_2 inner layer formed on the ablated surface. At this temperature, SiO_2 outer layer could protect the composites from corrosion effectively. In the transition region, with increasing temperature, SiO_2 outer layer was partly broke and ZrO_2–SiO_2 inner layer exposed to the oxyacetylene torch. In the center ablation region, SiO_2 layer lost its protective ability completely, and the molten ZrO_2 layer played a major role in protecting the C/C–ZrC–SiC composites from further ablation.

Acknowledgments

The work has been supported by the National Natural Science Foundation of China under Grant nos. 50832004 and 50972120, the Program of Introducing Talents of Discipline to University under Grant no. B08040, and financially supported by National "973" Project of the People's Republic of China, under Grant no. 2011CB605806.

References

[1] C.J. Li, A. Crosky, The effect of carbon fabric treatment on delamination of 2D-C/C composites, Composites Science and Technology 66 (2006) 2633–2638.

[2] Q.G. Fu, H.J. Li, Y.J. Wang, K.Z. Li, H. Wu, A Si–SiC oxidation protective coating for carbon/carbon composites prepared by a two-step pack cementation, Ceramics International 35 (2009) 2525–2529.

[3] X.H. Hou, H.J. Li, Y. Chen, K.Z. Li, Modeling of chemical vapor infiltration process for fabrication of carbon–carbon composites by finite difference methods, Carbon 37 (1999) 669–677.

[4] J.F. Huang, H.J. Li, X.R. Zeng, K.Z. Li, Yttrium silicate oxidation protective coating for SiC coated carbon/carbon composites, Ceramics International 32 (2006) 417–421.

[5] C. Vix-Guterl, C. Grotzinger, J. Dentzer, M.P. Bacosb, P. Ehrburger, Reactivity of a C/SiC composite in water vapour, Journal of the European Ceramic Society 21 (2001) 315–323.

[6] G.D. Li, X. Xiong, K.L. Huang, Ablation mechanism of TaC coating fabricated by chemical vapor deposition on carbon-carbon composites, Transactions of the Nonferrous Metals Society of China 19 (2009) s689–s695.

[7] Z.Q. Li, H.J. Li, W. Li, J. Wang, S.Y. Zhang, J. Guo, Preparation and ablation properties of ZrC–SiC coating for carbon/carbon composites by solid phase infiltration, Applied Surface Science 258 (2011) 565–571.

[8] D.D. Jayaseelan, R.G. Sá, P. Brown, W.E. Le, Reactive infiltration processing (RIP) of ultra high temperature ceramics (UHTC) into porous C/C composite tubes, Journal of the European Ceramic Society 31 (2011) 361–368.

[9] X.T. Li, J.L. Shi, G.B. Zhang, H. Zhang, Q.G. Guo, L. Liu, Effect of ZrB_2 on the ablation properties of carbon composites, Materials Letters 60 (2006) 892–896.

[10] Y.G. Wang, X.J. Zhu, L.T. Zhang, L.F. Cheng, Reaction kinetics and ablation properties of C/C–ZrC composites fabricated by reactive melt infiltration, Ceramics International 37 (2011) 1277–1283.

[11] X.T. Shen, K.Z. Li, H.J. Li, H.Y. Du, W.F. Cao, F.T. Lan, Microstructure and ablation properties of zirconium carbide doped carbon/carbon composites, Carbon 48 (2010) 344–351.

[12] Q.F. Tong, J.L. Shi, Y.Z. Song, Q.G. Guo, Resistance to ablation of pitch-derived ZrC/C composites, Carbon 42 (2004) 2495–2500.

[13] X.Q. Gao, L. Liu, Q.G. Guo, J.L. Shi, G.T. Zhai, The effect of zirconium addition on the microstructure and properties of chopped carbon fiber/carbon composites, Composites Science and Technology 67 (2007) 525–529.

[14] Q.G. Li, H.J. Zhou, S.M. Dong, Z. Wang, J.S. Yang, B. Wu, J.B. Hu, Fabrication and comparison of 3D C_f/ZrC–SiC composites using ZrC particles/polycarbosilane and ZrC precursor/polycarbosilane, Ceramics International 38 (2012) 5271–5275.

[15] H.T. Wu, X. Wei, S.Q. Yu., W.G. Zhang, Abalation performances of multi-phased C/C–ZrC–SiC ultra-high temperature composites, Journal of Inorganic Materials 26 (2011) 852–856.

[16] Q.G. Li, S.M. Dong, Z. Wang, P. He, H.J. Zhou, J.S. Yang, B. Wu, J.B. Hu, Fabrication and properties of 3-D C_f/SiC–ZrC composites, using ZrC precursor and polycarbosilane, Journal of the American Ceramic Society 95 (2012) 1216–1219.

[17] Z.J. Yu, L. Yang, J.Y. Zhan, C. Zhou, H. Min, Q. Zheng, H.P. Xia, Preparation, cross-linking and ceramization of AHPCS/Cp_2ZrCl_2 gybrid precursors for SiC/ZrC/C composites, Journal of the European Ceramic Society 32 (2012) 1291–1298.

[18] Measurement standard of ablation properties of materials, GJB323A-96, National Standard Committee of China, Beijing, 1996.

[19] G. Wen, S.H. Sui, L. Song, X.Y. Wang, L. Xia, Formation of ZrC ablation protective coatings on carbon material by tungsten inert gas cladding technique, Corrosion Science 52 (2010) 3018–3022.

[20] J. Han, P. Hu, X.H. Zhang, S.H. Meng, W.B. Han, Oxidation-resistant ZrB_2–SiC composites at 2200 °C, Composites Science and Technology 68 (2008) 799–806.

[21] E.L. Corral, L.S. Walker, Improved ablation resistance of C–C composites using zirconium diboride and boron carbide, Journal of the European Ceramic Society 30 (2010) 2357–2364.

[22] Z. Wang, Z.J. Wu, G.D. Shi, The oxidation behaviors of a ZrB_2–SiC–ZrC ceramic, Solid State Sciences 13 (2011) 534–538.

[23] H. Ping, G.L. Wang, W. Zhi, Oxidation mechanism and resistance of ZrB_2–SiC composites, Corrosion Science 51 (2009) 2724–2732.